

Zodiacal light observations and its link with cosmic dust: a review

Jeremie Lasue^a, Anny-Chantal Levasseur-Regourd^b, Jean-Baptiste Renard^c

^a*IRAP, Université de Toulouse, CNRS, CNES, UPS, 9 avenue Colonel Roche, FR-31400 Toulouse, France*

^b*LATMOS, Sorbonne Université, CNRS, UVSQ, Campus Pierre et Marie Curie, 4 place Jussieu, Paris FR-75005, Francee*

^c*LPC2E, CNRS, Orléans FR-45071, France*

Abstract

The zodiacal light is a night-glow mostly visible along the plane of the ecliptic. It represents the background radiation associated with solar light scattered by the tenuous flattened interplanetary cloud of dust particles surrounding the Sun and the planets. It is an interesting subject of study, as the source of the micrometeoroids falling on Earth, as a link to the activity of the small bodies of the Solar System, but also as a foreground that veils the low brightness extrasolar astronomical light sources.

In this review, we summarize the zodiacal light observations that have been done from the ground and from space in brightness and polarization at various wavelength ranges. Local properties of the interplanetary dust particles in some given locations can be retrieved from the inversion of the zodiacal light integrated along the light-of-sight. We show that the current community consensus favors that the majority of the interplanetary dust particles detected at 1 au originate from the activity of comets.

Our current understanding of the interplanetary dust particles properties is then discussed in the context of the recent results from the Rosetta rendezvous

*Corresponding author

Email address: jlasue@irap.omp.eu (Jeremie Lasue)

space mission with comet 67P/Churyumov-Gerasimenko.

Keywords: Zodiacal light, brightness, polarization, thermal emission, interplanetary dust, cometary dust

1. Introduction

The zodiacal light is a faint night-glow, brighter as the observer looks along the ecliptic and closer to the Sun. Its visual appearance usually takes the shape of Sun-colored cones of light visible at dusk and at dawn as illustrated in Fig. 1. In fact, the zodiacal light originates from the solar light scattered by the tenuous lenticular cloud of interplanetary dust particles surrounding the Sun and in which the planets orbit. Therefore, the study of its properties is of interest to better understand the origin and characteristics of interplanetary dust particles but also to better understand how planetary and exoplanetary systems evolve with time.

Figure 1: zodiacal light (ESO/Y.Beletsky)

The night sky brightness as seen from the ground on Earth originates from a combination of i. upper atmosphere airglow, ii. the zodiacal light scattered and emitted from the interplanetary dust particles in the solar system, iii. the integrated starlight from individual and unresolved stars, iv. the diffuse galactic light scattered from interstellar dust particles and emitted from the filamentary cirrus detected by IRAS (Hauser et al., 1984) and v. the extragalactic light and background (see e.g. Levasseur-Regourd, 1994). The first scientific work on the study of the zodiacal light was published by Cassini in the 17th century (Cassini, 1693). Scientists progressively understood that the light was present in every celestial direction, presented a solar spectrum, and was partially polarized. They therefore assumed it to be due to sunlight scattered by tiny solid particles (e.g. Wright, 1874). Quantitative measurements were pursued during

the 20th century with a view to better understand its constituting particles and to characterize this foreground signal to improve extrasolar astronomical observations. Extensive historical notes on the study of the zodiacal light can be found in e.g. Fechtig et al. (2001); Levasseur-Regourd et al. (2001).

The cloud’s brightness comes principally from scattering in the visible and by thermal emission in the infrared and so can be studied in both wavelength ranges. The most complete reviews of its properties were published almost 20 years ago in the report from the *IAU Commission 21: Light of the night sky* “The 1997 reference of diffuse night sky brightness” (Leinert et al., 1998) and in the “Interplanetary dust” book published in 2001 (Grün et al., 2001). Since then, a number of programs and space missions have improved the available measurements of the zodiacal light and our knowledge of the properties of the interplanetary dust particles that constitute it, like the space missions Solar Mass Ejection Imager (SMEI) in the visible (Buffington et al., 2016) and AKARI in the infrared (Pyo et al., 2010). In this work we will review the properties of the zodiacal light from observations and describe the properties of the interplanetary dust particles that can be deduced from them.

2. Integrated observations of the zodiacal light along the line of sight

2.1. Intensity observations

The initial studies of the zodiacal light originated from a need to better understand the solid matter environment surrounding the Earth, together with the fact that this glow was a source of noise to the study of faint objects and extended sources (see e.g. Dufay, 1925; Dumont, 1965; Leinert et al., 1998). The night sky brightness includes atmospheric glow, interplanetary dust light scattering and thermal emission, as well as galactic and extra-galactic point or diffuse sources. Long term surveys can disentangle these different signal

sources to retrieve each component separately. The study of the zodiacal light necessitates year-long surveys to obtain a full assessment of its geometry and determine possible time variations of the dust cloud.

The zodiacal light intensity, I , depends on the position of the observer along the terrestrial orbit, the wavelength and the viewing direction with respect to the Sun. The dust distribution around the Sun essentially follows a mirror symmetry with respect to a surface close to the ecliptic. This symmetry surface is close to a plane, but may diverge somewhat from it and is inclined by $i = 3.0^\circ \pm 0.3$ from the ecliptic plane as measured by the Helios probes between Earth and Venus orbits (Leinert et al., 1980). Helio-ecliptic coordinates, illustrated in Fig. 2, are generally suitable to describe the zodiacal light with the ecliptic latitude β and the helio-ecliptic longitude $(\lambda_e - \lambda_\odot)$, where λ_e is the ecliptic longitude. The phase angle of observation is noted α . As shown in Fig. 2, one needs to keep in mind that any signal observed in a given direction corresponds to an integrated signal along the line of sight.

Figure 2: geometry of observation

In the early years of space exploration a better understanding of the dust material surrounding the Earth was sought, and systematic observations of the zodiacal light were performed. High altitude surveys were performed with narrow filters to limit airglow contamination over several years in Hawaii (Weinberg, 1964). At the Canary Islands (Dumont, 1965) devised a method to remove the night airglow using a correlation between the 557.7 nm O I line and the atmospheric continuum observed on multiple points over the celestial sphere. Other astronomers' surveys were also compiled in Leinert (1975) and Fechtig et al. (1981), and include data obtained by Weinberg (1964); Blackwell et al. (1967a); Van de Noord (1970); Sparrow & Ney (1972); Leinert et al. (1976). Fig. 3 represents the zodiacal light signal averaged over a year in intensity, I , and linear

degree of polarization, P (which will be discussed in Section 2.2), on a diagram representing a quarter of the celestial sphere. The values presented correspond to the unification of the survey measurements published in tabular form in the review of Leinert et al. (1998). The outer circle represents the ecliptic. The minimum brightness is obtained at a point close to the ecliptic pole coordinates (Dumont & Sanchez, 1975a,b). Taking into account the fact that the zodiacal light has a solar spectrum, its intensity I at 550 nm is then found to be close to $2.4 \times 10^{-5} \text{ W m}^{-2} \text{ sr}^{-1} \mu\text{m}^{-1}$ at 30° solar elongation in the ecliptic plane (which outshines the brightest part of the Milky Way). It reaches a minimum of $7.6 \times 10^{-7} \text{ W m}^{-2} \text{ sr}^{-1} \mu\text{m}^{-1}$ in the vicinity of the ecliptic pole. In the ecliptic plane, a minimum of $1.8 \times 10^{-6} \text{ W m}^{-2} \text{ sr}^{-1} \mu\text{m}^{-1}$ is reached at around 140° , which is still 2.3 times higher than the ecliptic pole value. The resolution of the data is between 5° and 15° . The relative uncertainty in the intensity data remains below 5%. One notices the continuous decrease of I as the viewing direction moves away from the Sun, except for the direction directly opposite the Sun, named the *gegenschein*, where an increase in brightness is due to light backscattering and I reaches a value about 1.3 times larger than the ecliptic minimum.

Figure 3: Brightness and polarization maps

Meanwhile, several space mission observations were also obtained with the added advantage of not being contaminated by the atmospheric night-glow, but limited in viewing directions and mission time span. The characteristics of the dust were assessed in different zones of the Solar System thanks to their mobility. The D2A satellite around the Earth measured the zodiacal light in a plane perpendicular to the Sun-Earth direction. Its results confirmed the validity of ground-based measurements, and gave some evidence for the presence of interplanetary dust heterogeneities (Levasseur & Blamont, 1973). The Helios 1 and

2 probes showed an increase of I with decreasing heliocentric distance within the ecliptic plane (Leinert et al., 1981, 1982). This led to the assumption that the dust particles population density, n , was increasing towards the Sun as $n(r) \propto r^{-1.3}$, where r is the radial distance to the Sun. Toward the outer planets, observations were performed by Pioneer 10 and 11 (Hanner et al., 1976), establishing that the zodiacal light intensity decreases away from the Sun and becomes non detectable after 3 au (Matsumoto et al., 2018). These measurements confirmed and extended the surveys that were obtained from the ground.

For an observer located on Earth’s orbit, the zodiacal light intensity will vary depending on the distance to the Sun due to the Earth’s orbit eccentricity. Once this effect is corrected for, I observed at 1 au remains consistently stable within 1.5% over a whole solar cycle (Levasseur-Regourd, 1996). The remaining annual residual oscillations originate in a slight inclination of the zodiacal cloud’s symmetry plane with respect to the ecliptic. At 1 au, this symmetry plane presents an ascending node at $95^\circ \pm 20^\circ$ with an inclination of $1.5^\circ \pm 0.4^\circ$ (Dumont & Levasseur-Regourd, 1978). The symmetry surface of the zodiacal cloud is possibly warped far away from the Earth, as an inclination of about 3° was inferred from Helios measurements (Leinert et al., 1980) and a dust ring associated with the orbit of Venus detected (Leinert & Moster, 2007).

A re-analysis of Weinberg’s observations from Hawaii has recently yielded a new intensity map with a 2° resolution from which the ascending node position gives around 80° while the inclination of the cloud’s symmetry plane is around 2° (Kwon et al., 2004). Later on, the whole sky daily photometric observations by the Solar Mass Ejection Imager (SMEI) space mission were used to generate an even more precise and resolved zodiacal light map (Buffington et al., 2016). After image processing to remove the brightest stars, daily zodiacal maps with a resolution of 0.5° were calculated over the 8.5 years of the satellite mission

(from 2003 to 2011). An average zodiacal map is shown in Fig. 4 in the same reference frame as Fig. 3. Based on these measurements, an upper limit to the zodiacal light intensity changes of 0.3% was obtained for the time period of observations of 8.5 years. Using the same satellite data, (Buffington et al., 2009) determined that the *gegenschein* is always located at the anti-solar point, but varies by $\approx 10\%$ of its intensity over time, with a portion of the variation repeating seasonally. Similarly, the latest high-resolution (5' per pixel) survey of the *gegenschein* using a wide-angle camera showed that the maximum scattered intensity is consistently located at the anti-solar point. Ishiguro et al. (2013) fitted a model to the *gegenschein* geometry and constrained a very low albedo of 0.06 for the particles located in that direction.

Figure 4: Buffington zodiacal map

Local short-term enhancements in the zodiacal light brightness are also detected and were assumed to be due to possible meteoroid streams (e.g. Levasseur & Blamont, 1973). Since then the discovery of faint cometary trails in the infrared by the Infrared Astronomical Satellite (IRAS) (Sykes & Walker, 1992) and the Spitzer telescope (Reach et al., 2007) as well as linear dust features in the optical domain (Ishiguro et al., 1999; Yang et al., 2012) have clearly demonstrated the existence of many local enhancements in dust density due to the activity and impacts amongst the Solar System small bodies population (See e.g. Fig. 4 in Levasseur-Regourd & Lasue, 2019).

Extensive descriptions of the results and methods of zodiacal light surveys can be found in the reviews previously published (see Leinert, 1975; Weinberg & Sparrow, 1978; Leinert & Grün, 1990; Leinert et al., 1998; Levasseur-Regourd et al., 2001; Mann et al., 2004; Lasue et al., 2015)

2.2. Polarimetric properties

2.2.1. Degree of linear polarization observations

As light scattered by an optically thin cloud of dust particles, the zodiacal light presents a systematic linear polarization, P , defined as the ratio of the difference between the light intensity perpendicular, I_{\perp} , and parallel, I_{\parallel} , to the scattering plane and the total intensity $P = \frac{I_{\perp} - I_{\parallel}}{I_{\perp} + I_{\parallel}}$. The linear polarization P can reach values as high as 20% in the integrated line of sight. P is normalized and positive if the electric field polarization direction is perpendicular to the scattering plane as shown in Figure 2. Observations demonstrated that the majority of the night sky presents a positive linear polarization signal (Weinberg, 1985).

Fig. 3 bottom, represents the values of polarization annually averaged over the sky in differential ecliptic coordinates based on data from Dumont & Sanchez (1976) and Table 18 published in (Leinert et al., 1998). The error in the measured polarization is estimated to be $\approx 2\%$. The linear polarization is clearly dependent to the first order on the helio-ecliptic longitude. It decreases to zero towards the Sun, in the forward scattering direction, and reaches a maximum value of $\approx 20\%$ near 60° of helio-ecliptic longitude and near the ecliptic pole. The linear polarization signal then presents negative values around the *gegenschein* with a minimum of about -2% near 165° of elongation similar to the backscattering signal obtained with light scattered by irregular dust particles of sizes of the same order of magnitude as the light's wavelength, λ (Levasseur-Regourd et al., 1997; Lumme et al., 1997). While the negative value of polarization in that region of the sky may be difficult to correctly assess as discussed in (Dumont & Sanchez, 1975b), the presence of a negative polarization region surrounding the *gegenschein* was confirmed from measurements done on the ground Weinberg & Mann (1968), from sounding rockets Wolstencroft & Rose

(1967) as well as from balloons Frey et al. (1974), making it a robust detection. The inversion angle corresponds to $15^\circ \pm 5^\circ$, with a slope at inversion of (0.2 ± 0.1) percent per degree. Therefore the integrated linear polarization variation of the zodiacal light in the ecliptic plane follows variations similar to the ones of typical polarimetric phase curves of the Solar System small bodies surfaces (e.g., regolith on the Moon and on asteroids) or dust clouds (e.g., dust in cometary comae). This trend is typical of scattering by irregular particles, with a size greater than the wavelength ((Belskaya et al., 2019)).

Polarimetric observations have been done at different wavelengths and towards different directions of the sky as summarized in Fig. 5. There are no strong trends in the visible range, from 450 nm to 800 nm, but near infrared observations from 1 μm to 4 μm by COBE could indicate a decreasing trend towards higher wavelengths (Leinert et al., 1998). This could be due partly to contamination by the thermal dust emission, which starts at about 3 μm (Berriman et al., 1994). Also, because the observations summarized in Fig. 5 probe different regions of the zodiacal cloud complex, the scatterers must have different origins. As different spectral polarimetric trends are seen for different types of asteroidal surfaces (Belskaya et al., 2017) and cometary dust clouds (see e.g. Levasseur-Regourd et al., 1996; Hadamcik & Levasseur-Regourd, 2003) further more precise observations may indicate potential genetic links to the dust sources.

Figure 5: Spectral gradient for polarization

2.2.2. Solar F-corona observations

Closer to the Sun, the zodiacal cloud starts to merge with the solar corona. The brightness of the solar corona originates mainly from three physical processes: i. Thomson scattering by free electrons (K-corona, major component at < 4 solar radii), ii. line emission from ions (L-corona), and iii. light scattering

from dust particles (F-corona). The F-corona emission dominates at the largest distances and can be separated from the other emissions by spectrometric or polarimetric analyses.

The size range of observed particles may change in the F-corona compared to the zodiacal light, causing a change of their average optical properties. Typical sizes of the particles are still expected to remain larger than $1\ \mu\text{m}$ (Mann et al., 2004). The change in single particle scattering properties at small angles, however, is expected to change the radial slope of the F-coronal brightness compared to the zodiacal light. Combining overall measurements, it is expected that the brightness varies as $R^{-2.5}$ at the solar equator and $R^{-2.8}$ at the poles, with R the radial distance to the Sun (see Levasseur-Regourd et al., 2001, and references therein).

Color trends are not evidenced from measurements at wavelengths below $1\ \mu\text{m}$ (Kimura et al., 1998). At larger wavelengths, the F-corona brightness presents a reddening. The color is expected to vary within the corona as a result of the superposition of light scattering and thermal emission effects (Mann, 1993). Possible dust rings around the Sun in the region where material sublimation may occur were anticipated due to the balance between the inward Poynting-Robertson drag and the outward radiation pressure. Observations of the 1991 solar eclipse have shown no evidence for the existence of a dust ring around the Sun (see Levasseur-Regourd et al., 2001, and references therein).

Typical classical coronal models expect the F-corona polarization to decrease and tend to zero towards the Sun (Blackwell et al., 1967b). Polarimetric observations of the Solar corona (Skomorovsky et al., 2012; Burkepile et al., 2017) and data obtained by Clementine during solar occultations by the Moon (Hahn et al., 2002) have confirmed the variations measured in previous works (see reviews by Levasseur-Regourd et al., 2001; Mann et al., 2004).

2.2.3. Circular polarization

The light scattered by the interplanetary dust cloud is, to the first order, linearly polarized. However, multiple scattering, partial alignment of the dust particles, or even optically active materials can introduce a circular polarization component in the scattered light (see *e.g.* Mishchenko et al., 2002). Measurements of the circular polarization have been attempted from space and on the ground but remain inconclusive due to the very low level of signal expected (Wolstencroft & Rose, 1967; Staude & Schmidt, 1972; Wolstencroft & Kemp, 1972). Observations do not indicate circular polarization values in excess of 0.1% for most of the sky except for a possible signal in excess of 0.5% around a helio-ecliptic longitude of 240° (Wolstencroft & Kemp, 1972). In the case of the zodiacal cloud, one expects the major processes to explain a possible circular polarization to be either: i. particle alignment (Lazarian et al., 2015; Lasue et al., 2015), or ii. optically active materials. Both processes have been suggested to explain the very low circular polarization measured for comets with recent measurements by Rosetta favouring a particle alignment (Rosenbush et al., 2007; Kolokolova et al., 2016). Further attempts to observe the zodiacal light circular polarization may be of importance as it could constrain the origin of the particles and specific dynamic properties in the solar magnetic field.

2.3. Spectral properties

In the visible part of the spectrum, the zodiacal light shows a solar spectrum.

Looking at the spectral properties of the zodiacal light integrated along the line-of-sight at larger wavelengths, a number of interesting measurements have been performed, especially with space missions such as IRAS, COBE, ISO, AKARI, WISE and Planck, to deduce the physical properties and the dynamics of the dust particles in the interplanetary dust cloud.

First, many infrared measurements have put into evidence the presence of

dust trails and rings associated with the impacts of asteroids and the activity of comets (e.g. Dermott et al., 1984; Sykes, 1988; Reach, 1997) The spectral analysis of the Doppler shifted scattered solar light Fraunhofer lines gives insight into the dynamics of the dust particles constituting the zodiacal cloud. Ipatov et al. (2008) have shown the measurements to be consistent with a majority of the dust particles associated with cometary activity close to the Sun (< 1 au).

Then, a red spectral gradient of the scattered light is determined by many measurements in the range from 200 nm to $2\text{ }\mu\text{m}$, as shown by COBE (Berriman et al., 1994), and as summarized in (Leinert et al., 1998, and references therein). The spectral gradient can be calculated to be $S = 8.5 \pm 1.0\%/100\text{ nm}$ at 460 nm (Yang & Ishiguro, 2015). Combining this value with the albedo of $A = 0.06 \pm 0.01$ measured at the same wavelength in the direction of the *gegenschein* by Ishiguro et al. (2013) shows that such particles scattering properties are most consistent with the properties of primitive small bodies such as comets or D-type asteroids (Yang & Ishiguro, 2015).

Measurements (from balloons, rockets and satellites) of the thermal emission originating from the zodiacal cloud have also been performed. The zodiacal thermal emission, which gradually takes over the solar-spectrum by about $2\text{ }\mu\text{m}$, is actually the most prominent source of brightness in the 5 to 100 micrometer range, at least away from the galactic plane (e.g. Leinert et al., 1998). For even larger wavelengths, the sky brightness gets dominated by the interstellar medium, the cosmic diffuse infrared background and finally the cosmic microwave background.

This thermal range can be modelled using blackbody emission curves for specific mixtures of materials (like silicates, amorphous carbon and graphite). A change of slope in the spectrum at about $150\text{ }\mu\text{m}$ is interpreted to represent a change in the dust size distribution at a radius of about $30\text{ }\mu\text{m}$ (Fixsen & Dwek,

2002), which is consistent with the size distribution variations measured in situ (Grün et al., 1985). Comparison of the model with the data by Fixsen & Dwek (2002) indicates that replenishment of the interplanetary dust is $\approx 10^{11} \text{ kg yr}^{-1}$ from asteroids and comets. Dust emission rate from asteroids impacts and activity appears to be lower and thus, a significant contribution from comets would be needed to replenish the interplanetary dust cloud at 1 au.

The work by Reach et al. (2003) with the ISO satellite data also indicates a dust distribution dominated by large ($> 10 \mu\text{m}$ radius), low-albedo (< 0.08), rapidly-rotating, gray particles at 1 au from the Sun. Spectral signatures of amorphous and crystalline silicates are also detected in the infrared from 9 to $11 \mu\text{m}$ indicating also the presence of small particles similar to the ones ejected by active comets, such as C/1995 O1 Hale-Bopp comet, and to proto-planetary disks emission spectra. Similar spectral signatures of crystalline silicate features were obtained with the AKARI spacecraft (Ootsubo et al., 2009).

At even larger wavelengths, in the microwave domain, Planck measurements have shown that the zodiacal cloud is a minor correction to the Cosmic Microwave Background emission (Ade et al., 2014).

3. Interplanetary dust local properties from local inversion

So far, we have discussed only the properties of the zodiacal light, which is an integrated signal (Fig. 1) along the line of sight of the observer (Fig. 2). However, techniques have been tentatively developed to invert this signal in some cases, thus giving information on the local properties of the brightness and the polarization of the zodiacal light. This is what we describe in this section.

3.1. Inversion method

The dust in the zodiacal cloud cannot be assumed to have the same optical properties everywhere and in all directions. In the data integrated over the line of sight, contributions from light scattering by dust particles corresponding to different distances to the Sun, different observing phase angles and with likely different physical properties are mixed. In order to obtain specific properties of the dust particles, it is mandatory to invert the integrated intensity and polarization. Knowing that the zodiacal cloud is seen to be relatively homogeneous and in an apparent steady state, which is consistent with the mixing of injected dust particles and their short lifetimes (Campbell-Brown, 2008; Nesvorný et al., 2011; Yang & Ishiguro, 2018), it is possible to invert the light integrated over the line-of-sight to deduce local scattering properties of the dust particles. Local rigorous inversion and local inversions through mathematical methods are, together with their main results, summarized in Levasseur-Regourd et al. (2001), section 4.

Assuming that the zodiacal cloud has a plane of symmetry, within which the observer is located, and that the density of dust particles varies as a power-law with the heliocentric distance and is in an equilibrium state, a rigorous inversion of the zodiacal light intensity integrated along the line-of-sight can be derived from Earth-based observations as a function of the phase angle at 1 au (Dumont, 1973). Given the local values for the light intensity polarized parallel and perpendicular to the scattering plane, the associated local linear polarization can be directly calculated. This method is used to determine that at a phase angle $\alpha = 90^\circ$ at the symmetry plane, one cubic kilometer of interplanetary space scatters sunlight with an intensity that is 4×10^{-34} times smaller than the solar brightness (Schuerman, 1979). The local linear polarization is calculated to be about 0.30 ± 0.03 (Levasseur-Regourd et al., 1990).

Dumont (1983); Dumont & Levasseur-Regourd (1985) developed the method of the “nodes of lesser uncertainty” in order to invert the measurements outside the Earth’s orbital path. This method assumes rotational symmetry for the symmetry plane of the zodiacal cloud, a radial power-law decrease in the dust density from the Sun with a quasi-equilibrium state of the cloud density on the time-scale of a few weeks. Knowing that the local intensity scattering function is relatively smooth and regular, it can be represented by continuous mathematical functions (e.g. polynomials, or Fourier series) with five parameters out of which one is free. By using two lines of sight with solar elongations ϵ and $180^\circ - \epsilon$, these mathematical functions present two regions where the local brightness varies over a very limited range allowing to retrieve its value with a small uncertainty in those positions. These mathematical regions correspond to : i. the so-called “radial node”, located near the helio-ecliptic meridian with a variable solar distance, R , below 1 au and a constant phase angle, $\alpha = 90^\circ$, and ii. the so-called “martian node” located at a quasi-constant solar distance of $R \approx 1.5 \text{ au}$ but covering a phase angle range from 0° to 42° giving information on the backscattering function of the dust particles. Figure 6 illustrates the method and the position of the nodes. Note that the regions were named for illustration purposes but do not correspond to regions where measurements were done. They were retrieved with limited assumptions by mathematical inversion of the line of sight integral. Some further methods of inversion have also been devised to retrieve local contributions in the plane tangential to the Earth’s orbit, out of the ecliptic (Renard et al., 1995) and at other positions in the solar system (Schuerman, 1979). Improvements in the zodiacal light data collection will lead to further work on the local intensity and polarization characterization with a better spatial and angular resolution.

Figure 6: Observation geometry for zodiacal light inversion.

	Value at 1 au	Power law exponent (also called gradient)	Domain in au
Intensity	$\approx 23 \times 10^{-7}$ $\text{W m}^{-2} \text{ sr}^{-1} \mu\text{m}^{-1} \text{ rad}^{-1}$	-1.25 ± 0.02	0.5 to 1.4
Degree of linear polarization	$30 \pm 3 \%$	$+0.5 \pm 0.1$	0.5 to 1.4
Temperature	$250 \text{ K} \pm 10 \text{ K}$	-0.36 ± 0.03	1.1 to 1.4
Albedo	0.07 ± 0.03	-0.34 ± 0.05	1.1 to 1.4
Space density	$10^{-19} \text{ kg m}^{-3}$	-0.93 ± 0.07	1.1 to 1.4

Table 1: Variation of the local properties of the dust in the symmetry plane. The properties are described as a function of solar distance with a power law assumption. The optical properties (linear polarization, albedo, and intensity in $\text{W m}^{-2} \text{ sr}^{-1} \mu\text{m}^{-1} \text{ rad}^{-1}$ at 550 nm) are retrieved at $\alpha = 90^\circ$ (Levasseur-Regourd, 1996; Levasseur-Regourd et al., 2001). The density of the particles is inferred from the inverted values in intensity and polarization.

A summary of the local properties of the interplanetary dust (intensity, polarization, temperature, albedo, number density) in the symmetry plane as inverted from the data and at $\alpha = 90^\circ$ is presented in Table 1. The local values for the albedo at a given phase angle (around 90 degrees) is retrieved by combining the local values of the flux emission, the temperature and the intensity (Hanner et al., 1981).

3.2. Heliocentric variations

At the radial node, the inverted values for the local variation in intensity and polarization are presented in Fig. 6 at $\alpha = 90^\circ$ as a function of the heliocentric distance. The figure is expressed with the traditional zodiacal light brightness values given in $S_{10}(V)$, i.e. the equivalent number of 10^{th} visual magnitude solar type stars per square degree. This unit was historically useful since the zodiacal light presents a solar spectrum in the visible wavelengths and so was valid over the visual domain. While SI units, i.e., $\text{W m}^{-2} \text{ sr}^{-1} \mu\text{m}^{-1}$ are easier to understand, they nevertheless need to be associated to a precise wavelength ($1 S_{10}(V)$ is equal to $1.261 \times 10^{-8} \text{ W m}^{-2} \text{ sr}^{-1} \mu\text{m}^{-1}$ at 550 nm, see Levasseur-Regourd et al., 2001).

The brightness follows the power-law variation given in Table 1 and is con-

sistent with the local dust density distribution under a homogeneous zodiacal cloud hypothesis as described in Leinert et al. (1977). However, taking into account the variation in albedo with respect to the heliocentric distance gives a local dust particle density value following a power-law with an exponent of -0.93 ± 0.07 (significantly different from the -1.3 value obtained under the homogeneity assumption) (Levasseur-Regourd et al., 1991). The Poynting-Robertson effect predicts a $1/R$ dependence for the density of dust particles in circular orbits located within the region of production of dust particles (ranging from 0.1 au to about 10-20 au), which is consistent with the power-law coefficient thus determined (Hanner, 1980).

The degree of linear polarization, P , variation includes data obtained from a compilation by Fechtig et al. (1981), data inverted by Levasseur-Regourd (1996), data from the Dumont & Sanchez (1975b) survey and data observed close to the Sun inverted by Mann (1998). Numerical simulations from Lasue et al. (2007) and laboratory measurements from Hadamcik et al. (2018) are also superposed to the observations. P decreases with decreasing solar distance. The sharp decrease noticed below 0.3 au suggests that drastic changes to the dust particles properties take place closer to the Sun, in agreement with trends obtained in the F-corona (Mann & MacQueen, 1996).

The dust properties variation with the solar distance could be related to temporal evolution of the dust particles, with possible changes in their composition and/or their size distribution, as they spiral towards the Sun under the Poynting-Robertson effect and get progressively warmer. This will be discussed in Section 4.

Figure 7: Local brightness and polarimetric data

3.3. Phase angle variations

The local brightness and polarization phase curves of the zodiacal light at the martian node (≈ 1.5 au) are plotted in Fig. 7. One can notice that around the backscattering domain ($\alpha < 20^\circ$), the intensity decreases by 0.015 ± 0.05 magnitude per degree. This demonstrates the existence of an opposition effect for the interplanetary dust population (Muinonen & Lumme, 1991).

The overall shape of the polarization phase curve is smooth, with a slightly negative polarization in the backscattering region, an inversion angle around $(15 \pm 5)^\circ$ and a slope at inversion of (0.2 ± 0.1) percent per degree. This shape is typical of light interaction with irregular dust particles possibly in the shape of fluffy aggregates made of submicronic monomers (Levasseur-Regourd et al., 1997; Lumme et al., 1997). The behavior of both intensity and polarization phase curves is comparable to that of cometary dust or C-type asteroids.

The slope at inversion of the polarimetric phase curve can be related to the geometric albedo by the ‘Umov empirical law’ (Umov, 1905). From the inverted data, a geometric albedo value of 0.15 ± 0.08 can be calculated at 1 au (Levasseur-Regourd, 1998), which is consistent within the error bars with the value given in Table 1 and also consistent with the more recent analysis done by Ishiguro et al. (2013).

Finally, inversion of the local properties of the dust particles out of the symmetry plane of the zodiacal cloud in the plane perpendicular to the ecliptic and tangential to Earth’s orbit, have also been performed and normalized to the data inverted at 1 au and for $\alpha = 90^\circ$. The brightness decreases with the elevation, indicating a flattened geometry for the interplanetary dust cloud. The polarization also decreases with elevation by about 10% at 1 au while the albedo increases simultaneously from 0.8 to 0.11 (Renard et al., 1995). These variations can be explained by the presence of two contributing dust populations,

one coming from the asteroid belt and short period comets activity close to the ecliptic, and the other one, more isotropic, and originating from long period comets and with different properties.

Figure 8: Local brightness and polarimetric data

4. On the origins of interplanetary dust particles

4.1. Numerical and laboratory simulations

The intensity and polarization phase curves can be compared to numerical and experimental simulations in order to retrieve the likely physical properties of the scatterers.

A classical assumption, based on astronomical observations, is that interplanetary, cometary and interstellar dust particles consist of silicates, carbonaceous compounds and possibly ices (see e.g. Greenberg & Hage, 1990; Ehrenfreund et al., 2004). The optical indices of such materials would present both the possibility for high absorption (carbonaceous compounds and dirty ices) and for low absorption of light (pure ice and some silicates). Light scattering by irregular solid particles, especially micrometer-sized fluffy aggregates of submicrometer grains made of such materials are typically consistent with the intensity and polarization phase curves observed from interplanetary dust (Giese et al., 1978; Haudebourg et al., 1999; Nakamura & Okamoto, 1999). Furthermore, a red polarimetric color variation of the scattered light by irregular particles is linked to a lower porosity of the dust particles. It is therefore expected that compact dust particles, possibly in the shape of elongated spheroids to present less symmetries than spheres, could be significant contributors to the interplanetary dust distribution (Lasue et al., 2007; Kolokolova & Kimura, 2010).

As shown in Fig. 7, the variation in local scattered intensity and polarization gives information on the heliocentric changes in dust density and properties. To

the first order, the scattered intensity can be explained by the dust density variation consistent with the Poynting-Robertson effect.

From numerical simulations in Lasue et al. (2007), that have been confirmed by laboratory simulations (Hadamcik et al., 2018), the decrease in polarization sunward around 1 au can be explained to first order by a change in the optical index of the dust particles population scattering the light. In that hypothesis, the proportion of absorbing materials, such as carbonaceous compounds, to weakly absorbing ones would decrease sensibly towards the Sun (from 50-100% at 1.5 au to about 0% at 0.6 au). A plot of the numerical simulations and experimental measurements data points are shown on Fig. 7b. This explanation would be consistent with an increase in the dust population albedo sunward, which is expressed by the variation equation shown for the albedo in Tab. 1. Other changes in the dust population properties may also occur.

Still in Fig. 7, closer to the Sun, below 0.3 au, one notices a sharp decrease in polarization as well as a change of slope in the scattered intensity. This change in behavior indicates that some properties of the dust cloud (size distribution, morphology, composition, etc.) is abruptly changing in that region. Many materials may sublime in that region and are certainly contributors to changes in either size distribution, shape or optical indices of the dust particles (Mann et al., 2004).

As interplanetary dust particles spiral inwards and vanish in the Sun, with a typical lifetime of a couple of million years at 1 au (Burns et al., 1979), the interplanetary dust cloud requires constant replenishment. Comet nuclei activity as well as asteroidal collisions in the Main Belt can provide substantial amounts of dust particles and have long been considered to be major contributors to the inner zodiacal cloud (Whipple, 1950; Dermott et al., 1984). Other minor contributions come from the giant planets environment, the Kuiper Belt, and

from interstellar dust particles (see e.g. Grün et al., 1993). Observations of the visual zodiacal intensity within 1 au by the Clementine space probe fitted with a model of dust distribution including asteroids, Jupiter Family Comets (JFC), Halley-type comets and Oort cloud comets indicates that at least 89% of the interplanetary dust located in a sphere within 1 au from the Sun originate from comets (Hahn et al., 2002). Numerical simulations of the IRAS observations in the thermal domain of the zodiacal cloud based on the dynamical properties of the dust ejected from comets and from asteroids indicates that 85-95% of the mid-infrared emission visible from 1 au is produced by JFCs, while asteroidal and long-period comets are both respectively smaller than 10% (Nesvorný et al., 2010, 2011). Similar conclusions are reached with the dynamical study of the evolution of aggregate dust particles injected in the inner solar system by active comets and with a size frequency distribution like the one of 67P/Churyumov-Gerasimenko, as they can reproduce the interplanetary dust properties detected around the Earth’s orbit (Yang & Ishiguro, 2018). Consistent results were also obtained from the study of the Doppler shift from the Fraunhofer lines of the scattered solar light (Ipatov et al., 2008). An improved model of the IRAS and COBE thermal emission observations by Rowan-Robinson & May (2013) determined similar numbers with, in addition, less than 1% interstellar dust contribution at 1 au. Finally, lidar observations of Na and Fe fluxes in the Earth’s atmosphere coupled with the cosmic spherule accretion rate measured at the South Pole also indicates that JFCs contribute $87 \pm 17\%$ of the total extraterrestrial matter mass input on the Earth (Carrillo-Sánchez et al., 2016).

In summary, based on those diverse lines of evidence, and others described in the previous sections, a consensus appears to emerge that the majority of the dust particles located within 1 au should be contributed from the activity of comets, and in particular the JFCs.

4.2. Properties of interplanetary dust and their link with comets

As we have seen above, the dust particles at the origin of the zodiacal light are expected to present specific characteristics based on the properties of the scattered and emitted zodiacal light in the visible and the thermal wavelengths. Several lines of evidence based on different arguments make a compelling case to link the properties of the interplanetary dust particles to those of cometary dust particles.

First, the dust density distribution models and related dynamics indicate that the majority of dust particles within 1 au from the Sun probably originate in major part from the activity of short period comets. This observation is also consistent with some of the properties detected for the meteoroids population impacting the Earth. For example, almost all meteor showers have been linked with cometary parent bodies (Jenniskens, 2006). The properties of interplanetary dust particles collected in the stratosphere of the Earth by airplanes are also consistent with primitive material and represent a family of samples that are chemically unlike the extraterrestrial matter represented by the meteorites (originating from asteroids apart from possibly one or two exceptions) (Flynn et al., 2016; Koschny et al., 2019). A population of micrometeorites named as UCAMM (Ultra-Carbonaceous Antarctic MicroMeteorites) for their very high carbon content (from 48% to 85%) has also been studied and present a D/H ratio more than one order of magnitude larger than the terrestrial values strongly suggesting a cometary origin (Duprat et al., 2010).

Second, the properties of the zodiacal light are consistent with a mixture of irregular fluffy particles and compact particles formed of silicates and carbonaceous materials. These properties are consistent with the properties of interplanetary dust collected in the stratosphere (Flynn et al., 2016). They are also coherent with the properties of cometary dust particles as observed from the

ground, analyzed in situ by sample return from Stardust and more recently from the in situ analysis performed by the Rosetta space mission (see e.g. Levasseur-Regourd et al., 2018). Most notably, the presence of both fluffy aggregates of grains and compact particles have been evidenced by both Stardust and Rosetta space missions (Hörz et al., 2006; Güttler et al., 2019). Similarly, both the Stardust samples and the Rosetta measurements have shown a distinct population of carbonaceous material forming a major fraction of the ejected dust with characteristics different from meteorites and possibly atmospheric IDPs (Sandford et al., 2006; Fray et al., 2016). Finally, the scattered light phase curves present a similar behavior between ejected cometary dust and interplanetary dust particles analogues (Levasseur-Regourd et al., 2019).

Overall the study of the zodiacal light can give us access to properties of the cometary particles that may not be accessible by other means, since samples that arrive on Earth may be biased, and cometary space missions are limited in numbers. Continued monitoring of the zodiacal light over time will provide a better understanding of the origin and evolution of the interplanetary dust environment. Going one step further, the study of the similarities between the light scattering behavior of interplanetary dust particles, asteroids, cometary dust clouds and protoplanetary disks will help us understand planetary formation processes and the origin of the solid particles in these different environments (Levasseur-Regourd et al., 2020).

5. Conclusions and future observations

In this work, we attempted to give an overview of the properties of the zodiacal light and its link with the physical properties of the interplanetary dust particles that evolve in the Solar System and their sources. The zodiacal light observations provide us with an overall picture of the interplanetary

dust environment: its mass flux distribution; chemical, material and structural properties; and the importance of different cometary and asteroidal sources in populating the inner Solar System with dust. This information has implications for the determination of the meteoroid flux deposited over the planetary surfaces.

Intensity and polarization values of the zodiacal light are also of major importance for outer Solar System observations, since they provide an estimate of the foreground noise induced by the zodiacal light, together with an optimization of the epochs of observations of faint extended astronomical objects (Leinert et al., 1998; Levasseur-Regourd & Lasue, 2019)

We can expect the next generations of sensitive whole sky surveys to provide many additional constraints on the zodiacal light with the possible detection of additional local heterogeneities and global time variability. Such surveys will include ground-based telescopes such as the Large Synoptic Survey Telescope (LSST), an optical 8.4m telescope designed to survey the visible sky every week starting in 2020 (Abell et al., 2009), but also space missions such as the Messier mission, a space telescope that will scan the night sky in the 200-1000 nm range, reaching surface brightness levels of 34 and 37 mag arcsec⁻² in the UV and optical domains (Valls-Gabaud & collaboration, 2016; Muslimov et al., 2017). These results will need to be compared with the results obtained by the space missions studying the small bodies of the Solar System, such as Hayabusa2 and OSIRIS-REx missions for asteroids and the newly selected ESA Comet Interceptor mission to flyby a new pristine active comet (Gater, 2019). Further data out of the Earth’s orbit could be obtained closer to the Sun from the recently launched Parker Solar Probe, and by other probes tangentially to the orbits of planets or small bodies they may be orbiting. Also, future observations of the zodiacal light may be sensitive to circular polarization, which could constrain

the origin of the particles and specific dynamic properties in the solar magnetic field.

Some important unsolved questions related to the zodiacal light that need to be studied in the future include:

- the exact origin and physical properties of the dust particles contributing to the zodiacal cloud,
- the possible time evolution of the zodiacal cloud over decades,
- the circular polarization that can probe the interplanetary magnetic field structures,
- the dust evolution in the vicinity of the Sun.
- how the properties of the zodiacal cloud could help us constrain the properties of exo-zodiacal dust clouds, which may behave quite differently depending on the presence and the properties of orbiting exoplanets.

Answers will progressively be found as future observations continue to focus on higher resolution photopolarimetry of the zodiacal light at all wavelengths and possibly observed out of the ecliptic. Improvements on the inversion methods based on such measurements will also likely further improve zodiacal light studies.

6. Acknowledgements

This work was supported by the Programme National de Planétologie (PNP) of CNRS/INSU, co-funded by CNES. We acknowledge the organizers of the Meteoroids 2019 conference for inviting the authors to present this work. We thank two anonymous referees for providing interesting discussions and improvements on the manuscript.

References

- Abell, P. A., Burke, D. L., Hamuy, M., Nordby, M., Axelrod, T. S., Monet, D., Vrsnak, B., Thorman, P., Ballantyne, D. R., & Simon, J. D. (2009). *LSST science book, version 2.0*. Technical Report FERMILAB-TM-2495-A, SLAC-R-1031. URL: <http://www.lsst.org/lsst/scibook>.
- Ade, P. A., Aghanim, N., Armitage-Caplan, C., Arnaud, M., Ashdown, M., Atrio-Barandela, F., Aumont, J., Baccigalupi, C., Banday, A. J., & Barreiro, R. B. (2014). Planck 2013 results. XIV. Zodiacal emission. *Astronomy & Astrophysics*, *571*, A14.
- Belskaya, I., Cellino, A., Levasseur-Regourd, A.-C., & Bagnulo, S. (2019). Optical Polarimetry of Small Solar System Bodies: From Asteroids to Debris Disks. In *Astronomical Polarisation from the Infrared to Gamma Rays* (pp. 223–246). Springer.
- Belskaya, I. N., Fornasier, S., Tozzi, G. P., Gil-Hutton, R., Cellino, A., Antonyuk, K., Krugly, Y. N., Dovgopol, A. N., & Faggi, S. (2017). Refining the asteroid taxonomy by polarimetric observations. *Icarus*, *284*, 30–42.
- Berriman, G. B., Boggess, N. W., Hauser, M. G., Kelsall, T., Lisse, C. M., Moseley, S. H., Reach, W. T., & Silverberg, R. F. (1994). COBE DIRBE near-infrared polarimetry of the zodiacal light: Initial results. *The Astrophysical Journal*, *431*, L63–L66.
- Blackwell, D. E., Dewhirst, D. W., & Ingham, M. F. (1967a). The zodiacal light. In *Advances in Astronomy and Astrophysics* (pp. 1–69). Elsevier volume 5.
- Blackwell, D. E., Ingham, M. F., & Petford, A. D. (1967b). The distribution of dust in interplanetary space. *Monthly Notices of the Royal Astronomical Society*, *136*, 313–328.

- Buffington, A., Bisi, M. M., Clover, J. M., Hick, P. P., Jackson, B. V., Kuchar, T. A., & Price, S. D. (2009). Measurements of the gegenschein brightness from the Solar Mass Ejection Imager (SMEI). *Icarus*, *203*, 124–133.
- Buffington, A., Bisi, M. M., Clover, J. M., Hick, P. P., Jackson, B. V., Kuchar, T. A., & Price, S. D. (2016). Measurements and an empirical model of the Zodiacal brightness as observed by the Solar Mass Ejection Imager (SMEI). *Icarus*, *272*, 88–101.
- Burkepile, J., Boll, A., Casini, R., de Toma, G., Elmore, D. F., Gibson, K. L., Judge, P. G., Mitchell, A. M., Penn, M., & Sewell, S. D. (2017). Polarization observations of the total solar eclipse of August 21, 2017. In *AGU Fall Meeting Abstracts*.
- Burns, J. A., Lamy, P. L., & Soter, S. (1979). Radiation forces on small particles in the solar system. *Icarus*, *40*, 1–48.
- Campbell-Brown, M. D. (2008). High resolution radiant distribution and orbits of sporadic radar meteoroids. *Icarus*, *196*, 144–163.
- Carrillo-Sánchez, J. D., Nesvorný, D., Pokorný, P., Janches, D., & Plane, J. M. C. (2016). Sources of cosmic dust in the Earth’s atmosphere. *Geophysical Research Letters*, *43*, 11–979.
- Cassini, G. D. (1693). Découverte de la lumière celeste qui paroist dans le zodiaque. *Mémoires de l’Académie Royale des Sciences*, *637*.
- Dermott, S. F., Nicholson, P. D., Burns, J. A., & Houck, J. R. (1984). Origin of the solar system dust bands discovered by IRAS. *Nature*, *312*, 505–509.
- Dufay, J. (1925). La polarisation de la lumière zodiacale. *CR Acad. Sc. Paris*, *181*, 399–401.

- Dumont, R. (1965). Séparation des composantes atmosphériques et interplanétaire et stellaire du ciel nocturne à 5000 Å. Applications à la photométrie de la lumière zodiacale et du Gegenschein. In *Annales d'Astrophysique* (pp. 265–313). CNRS volume 28.
- Dumont, R. (1973). Phase function and polarization curve of interplanetary scatterers from zodiacal light photopolarimetry. *Planetary and Space Science*, *21*, 2149–2155.
- Dumont, R. (1983). Zodiacal light gathered along the line of sight: The vicinity of the terrestrial orbit studied with photopolarimetry and with Doppler spectrometry. *Planetary and Space Science*, *31*, 1381–1387.
- Dumont, R., & Levasseur-Regourd, A. C. (1978). Zodiacal light photopolarimetry. IV-Annual variations of brightness and the symmetry plane of the zodiacal cloud: Absence of solar-cycle variations. *Astronomy & Astrophysics*, *64*, 9–16.
- Dumont, R., & Levasseur-Regourd, A. C. (1985). Zodiacal Light gathered along the line of sight: Retrieval of the local scattering coefficient from photometric surveys of the ecliptic plane. *Planetary and Space Science*, *33*, 1–9.
- Dumont, R., & Sanchez, F. (1975a). Zodiacal light photopolarimetry. I- Observations, reductions, disturbing phenomena, accuracy. II-Gradients along the ecliptic and the phase functions of interplanetary matter. *Astronomy & Astrophysics*, *38*, 397–403.
- Dumont, R., & Sanchez, F. (1975b). Zodiacal light photopolarimetry. II. Gradients along the ecliptic and the phase functions of interplanetary matter. *Astronomy & Astrophysics*, *38*, 405–412.
- Dumont, R., & Sanchez, F. (1976). Zodiacal light photopolarimetry. III-All-sky

- survey from Teide 1964-1975 with emphasis on off-ecliptic features. *Astronomy & Astrophysics*, 51, 393–399.
- Duprat, J., Dobrică, E., Engrand, C., Aléon, J., Marrocchi, Y., Mostefaoui, S., Meibom, A., Leroux, H., Rouzaud, J.-N., & Gounelle, M. (2010). Extreme deuterium excesses in ultracarbonaceous micrometeorites from central Antarctic snow. *Science*, 328, 742–745.
- Ehrenfreund, P., Charnley, S. B., & Wooden, D. H. (2004). From interstellar material to cometary particles and molecules. *Comets II*, (pp. 115–133).
- Fechtig, H., Leinert, C., & Berg, O. E. (2001). Historical perspectives. In *Interplanetary dust* (pp. 1–55). Springer.
- Fechtig, H., Leinert, C., & Grün, E. (1981). Interplanetary dust and zodiacal light. In *Landolt-Bornstein Numerical Data and Functional Relationships in Science and Technology* (p. 228). Springer-Verlag Heidelberg volume 2.
- Fixsen, D. J., & Dwek, E. (2002). The zodiacal emission spectrum as determined by COBE and its implications. *The Astrophysical Journal*, 578, 1009–1014.
- Flynn, G. J., Nittler, L. R., & Engrand, C. (2016). Composition of cosmic dust: sources and implications for the early solar system. *Elements*, 12, 177–183.
- Fray, N., Bardyn, A., Cottin, H., Altwegg, K., Baklouti, D., Briois, C., Colangeli, L., Engrand, C., Fischer, H., & Glasmachers, A. (2016). High-molecular-weight organic matter in the particles of comet 67P/Churyumov–Gerasimenko. *Nature*, 538, 72–74.
- Frey, A., Hofmann, W., Lemke, D., & Thum, C. (1974). Photometry of the zodiacal light with the balloon-borne telescope THISBE. *Astronomy and Astrophysics*, 36, 447–454.

- Gater, W. (2019). Comet mission given green light by European Space Agency. *Physics World*, 32, 13.
- Giese, R. H., Weiss, K., Zerull, R. H., & Ono, T. (1978). Large fluffy particles-A possible explanation of the optical properties of interplanetary dust. *Astronomy & Astrophysics*, 65, 265–272.
- Greenberg, J. M., & Hage, J. I. (1990). From interstellar dust to comets-A unification of observational constraints. *Astrophysical Journal*, 361, 260–274.
- Grün, E., Gustafson, B. A., Dermott, S., & Fechtig, H. (2001). *Interplanetary dust*. Springer Science & Business Media.
- Grün, E., Zook, H. A., Baguhl, M., Balogh, A., Bame, S. J., Fechtig, H., Forsyth, R., Manner, M. S., Horanyi, M., & Kissel, J. (1993). Discovery of Jovian dust streams and interstellar grains by the Ulysses spacecraft. *Nature*, 362, 428–430.
- Grün, E., Zook, H. A., Fechtig, H., & Giese, R. H. (1985). Collisional balance of the meteoritic complex. *Icarus*, 62, 244–272.
- Güttler, C., Mannel, T., Rotundi, A., Merouane, S., Fulle, M., Bockelée-Morvan, D., Lasue, J., Levasseur-Regourd, A. C., Blum, J., Naletto, G., Sierks, H., Hilchenbach, M., Tubiana, C., Capaccioni, F., Paquette, J. A., Flandes, A., Moreno, F., Agarwal, J., Bodewits, D., Bertini, I., Tozzi, G. P., Hornung, K., Langevin, Y., Krüger, H., Longobardo, A., Corte, V. D., Tóth, I., Filacchione, G., Ivanovski, S. L., Mottola, S., & Rinaldi, G. (2019). Synthesis of the morphological description of cometary dust at comet 67P/Churyumov-Gerasimenko. *Astronomy & Astrophysics*, 630, A24. doi:10.1051/0004-6361/201834751.
- Hadamcik, E., Lasue, J., Levasseur-Regourd, A. C., & Renard, J.-B. (2018).

- Analogues of interplanetary dust particles to interpret the zodiacal light polarization. *Planetary and Space Science*, . doi:10.1016/j.pss.2018.04.022.
- Hadamcik, E., & Levasseur-Regourd, A. C. (2003). Dust evolution of comet C/1995 O1 (Hale-Bopp) by imaging polarimetric observations. *Astronomy & Astrophysics*, *403*, 757–768.
- Hahn, J. M., Zook, H. A., Cooper, B., & Sunkara, B. (2002). Clementine observations of the zodiacal light and the dust content of the inner solar system. *Icarus*, *158*, 360–378.
- Hanner, M. S. (1980). On the albedo of the interplanetary dust. *Icarus*, *43*, 373–380.
- Hanner, M. S., Giese, R. H., Weiss, K., & Zerull, R. (1981). On the definition of albedo and application to irregular particles. *Astronomy & Astrophysics*, *104*, 42–46.
- Hanner, M. S., Sparrow, J. G., Weinberg, J. L., & Beeson, D. E. (1976). 1.1. 4 Pioneer 10 Observations of Zodiacal Light Brightness near the Ecliptic: Changes with Heliocentric Distance. In *International Astronomical Union Colloquium* (pp. 29–35). Cambridge University Press volume 31.
- Haudebourg, V., Cabane, M., & Levasseur-Regourd, A.-C. (1999). Theoretical polarimetric responses of fractal aggregates, in relation with experimental studies of dust in the solar system. *Physics and Chemistry of the Earth, Part C: Solar, Terrestrial & Planetary Science*, *24*, 603–608.
- Hauser, M. G., Gillett, F. C., Low, F. J., Gautier, T. N., Beichman, C. A., Neugebauer, G., Aumann, H. H., Baud, B., Boggess, N., & Emerson, J. P. (1984). IRAS observations of the diffuse infrared background. *The Astrophysical Journal*, *278*, L15–L18.

- Hörz, F., Bastien, R., Borg, J., Bradley, J. P., Bridges, J. C., Brownlee, D. E., Burchell, M. J., Chi, M., Cintala, M. J., & Dai, Z. R. (2006). Impact features on Stardust: Implications for comet 81P/Wild 2 dust. *Science*, *314*, 1716–1719.
- Ipatov, S. I., Kuttyrev, A. S., Madsen, G. J., Mather, J. C., Moseley, S. H., & Reynolds, R. J. (2008). Dynamical zodiacal cloud models constrained by high resolution spectroscopy of the zodiacal light. *Icarus*, *194*, 769–788.
- Ishiguro, M., Nakamura, R., Fujii, Y., Morishige, K., Yano, H., Yasuda, H., Yokogawa, S., & Mukai, T. (1999). First detection of visible zodiacal dust bands from ground-based observations. *The Astrophysical Journal*, *511*, 432–435.
- Ishiguro, M., Yang, H., Usui, F., Pyo, J., Ueno, M., Ootsubo, T., Kwon, S. M., & Mukai, T. (2013). High-resolution imaging of the gegenschein and the geometric albedo of interplanetary dust. *The Astrophysical Journal*, *767*, 75 (13pp).
- Jenniskens, P. (2006). *Meteor showers and their parent comets*. Cambridge University Press.
- Kimura, H., Mann, I., & Mukai, T. (1998). Influence of dust shape and material composition on the solar F-corona. *Planetary and Space Science*, *46*, 911–919.
- Kolokolova, L., & Kimura, H. (2010). Effects of electromagnetic interaction in the polarization of light scattered by cometary and other types of cosmic dust. *Astronomy & Astrophysics*, *513*, A40.
- Kolokolova, L., Koenders, C., Goetz, C., Rosenbush, V., Kiselev, N., Hoang, T., & Lazarian, A. (2016). Clues to cometary circular polarization from studying the magnetic field in the vicinity of the nucleus of comet

- 67P/Churyumov–Gerasimenko. *Monthly Notices of the Royal Astronomical Society*, 462, S422–S431.
- Koschny, D., Soja, R. H., Engrand, C., Flynn, G. J., Lasue, J., Levasseur-Regourd, A.-C., Malaspina, D., Nakamura, T., Poppe, A. R., & Sterken, V. J. (2019). Interplanetary Dust, Meteoroids, Meteors and Meteorites. *Space Science Reviews*, 215, 34.
- Kwon, S. M., Hong, S. S., & Weinberg, J. L. (2004). An observational model of the zodiacal light brightness distribution. *New Astronomy*, 10, 91–107.
- Lasue, J., Levasseur-Regourd, A. C., Fray, N., & Cottin, H. (2007). Inferring the interplanetary dust properties-from remote observations and simulations. *Astronomy & Astrophysics*, 473, 641–649.
- Lasue, J., Levasseur-Regourd, A. C., & Lazarian, A. (2015). Polarimetry of the interplanetary dust cloud. In L. Kolokolova, J. Hough, & A. C. Levasseur-Regourd (Eds.), *Polarization of stars and planetary systems* (pp. 419–436). Cambridge University Press.
- Lazarian, A., Andersson, B. G., & Hoang, T. (2015). Grain Alignment: Role of Radiative Torques and Paramagnetic Relaxation. In L. Kolokolova, J. Hough, & A. C. Levasseur-Regourd (Eds.), *Polarization of stars and planetary systems* (pp. 81–112). Cambridge University Press.
- Leinert, C. (1975). Zodiacal light—a measure of the interplanetary environment. *Space Science Reviews*, 18, 281–339.
- Leinert, C., Bowyer, S., Haikala, L. K., Hanner, M. S., Hauser, M. G., Levasseur-Regourd, A.-C., Mann, I., Mattila, K., Reach, W. T., & Schlosser, W. (1998). The 1997 reference of diffuse night sky brightness. *Astronomy & Astrophysics Supplement Series*, 127, 1–99.

- Leinert, C., & Grün, E. (1990). Interplanetary dust. In *Physics of the inner heliosphere I* (pp. 207–275). Springer.
- Leinert, C., Hanner, M., Richter, I., & Pitz, E. (1980). The plane of symmetry of interplanetary dust in the inner solar system. *Astronomy & Astrophysics*, *82*, 328–336.
- Leinert, C., Link, H., Pitz, E., & Giese, R. H. (1976). Interpretation of a rocket photometry of the inner zodiacal light. *Astronomy & Astrophysics*, *47*, 221–230.
- Leinert, C., & Moster, B. (2007). Evidence for dust accumulation just outside the orbit of Venus. *Astronomy & Astrophysics*, *472*, 335–340.
- Leinert, C., Pitz, E., Hanner, M., & Link, H. (1977). Observations of zodiacal light from Helios 1 and 2. *Journal of Geophysics Zeitschrift Geophysik*, *42*, 699–704.
- Leinert, C., Richter, I., Pitz, E., & Hanner, M. (1982). Helios zodiacal light measurements-a tabulated summary. *Astronomy & Astrophysics*, *110*, 355–357.
- Leinert, C., Richter, I., Pitz, E., & Planck, B. (1981). The zodiacal light from 1.0 to 0.3 AU as observed by the Helios space probes. *Astronomy & Astrophysics*, *103*, 177–188.
- Levasseur, A. C., & Blamont, J. E. (1973). Satellite observations of intensity variations of the zodiacal light. *Nature*, *246*, 26–28.
- Levasseur-Regourd, A. C. (1994). Natural Background Radiation-the Light from the Night Sky. In D. McNally (Ed.), *The Vanishing Universe: Adverse Environmental Impacts on Astronomy* (p. 64). New-York: Cambridge University Press.

- Levasseur-Regourd, A. C. (1996). Optical and thermal properties of zodiacal dust. In *International Astronomical Union Colloquium* (pp. 301–308). Cambridge University Press volume 150.
- Levasseur-Regourd, A. C. (1998). Zodiacal light, certitudes and questions. *Earth, Planets and Space*, *50*, 607–610.
- Levasseur-Regourd, A. C., Agarwal, J., Cottin, H., Engrand, C., Flynn, G., Fulle, M., Gombosi, T., Langevin, Y., Lasue, J., & Mannel, T. (2018). Cometary dust. *Space Science Reviews*, *214*, 64.
- Levasseur-Regourd, A. C., Baruteau, C., Lasue, J., Milli, J., & Renard, J.-B. (2020). Linking studies of micrometeoroids, zodiacal dust, cometary dust and circumstellar disks. *Planetary and Space Science*, . doi:10.1016/j.pss.2020.104896.
- Levasseur-Regourd, A. C., Cabane, M., Worms, J. C., & Haudebourg, V. (1997). Physical properties of dust in the solar system: relevance of a computational approach and of measurements under microgravity conditions. *Advances in Space Research*, *20*, 1585–1594.
- Levasseur-Regourd, A. C., & Dumont, R. (1980). Absolute photometry of zodiacal light. *Astronomy & Astrophysics*, *84*, 277–279.
- Levasseur-Regourd, A. C., Dumont, R., & Renard, J.-B. (1990). A comparison between polarimetric properties of cometary dust and interplanetary dust particles. *Icarus*, *86*, 264–272.
- Levasseur-Regourd, A. C., Hadamcik, E., & Renard, J.-B. (1996). Evidence for two classes of comets from their polarimetric properties at large phase angles. *Astronomy & Astrophysics*, *313*, 327–333.

- Levasseur-Regourd, A. C., & Lasue, J. (2019). Progresses in zodiacal light understanding: Significance for faint extended sources and clues for Solar System evolution. *Proceedings IAU Symposium The Realm of the Low-Surface-Brightness Universe*, 355.
- Levasseur-Regourd, A. C., Mann, I., Dumont, R., & Hanner, M. S. (2001). Optical and thermal properties of interplanetary dust. In E. Grün, B. A. S. Gustafson, S. F. Dermott, & H. Fechtig (Eds.), *Interplanetary dust* (pp. 57–94). Springer.
- Levasseur-Regourd, A. C., Renard, J. B., & Dumont, R. (1991). The zodiacal cloud complex. In *Origin and evolution of interplanetary dust* (pp. 131–138). Springer.
- Levasseur-Regourd, A. C., Renard, J.-B., Hadamcik, E., Lasue, J., Bertini, I., & Fulle, M. (2019). Interpretation through experimental simulations of phase functions revealed by Rosetta in 67P dust coma. *Astronomy & Astrophysics*, 630, A20. doi:10.1051/0004-6361/201834894.
- Lumme, K., Rahola, J., & Hovenier, J. W. (1997). Light scattering by dense clusters of spheres. *Icarus*, 126, 455–469.
- Mann, I. (1993). The influence of circumsolar dust on the whitelight corona—study of the visual F-corona brightness. *Planetary and space science*, 41, 301–305.
- Mann, I. (1998). Zodiacal cloud complexes. *Earth, planets and space*, 50, 465–471.
- Mann, I., Kimura, H., Biesecker, D. A., Tsurutani, B. T., Grün, E., McKibben, R. B., Liou, J.-C., MacQueen, R. M., Mukai, T., & Guhathakurta, M. (2004). Dust near the Sun. *Space Science Reviews*, 110, 269–305.

- Mann, I., & MacQueen, R. M. (1996). Observation and analysis of the F-corona brightness. *Advances in Space Research*, *17*, 53–56.
- Matsumoto, T., Tsumura, K., Matsuoka, Y., & Pyo, J. (2018). Zodiacal light beyond earth orbit observed with Pioneer 10. *The Astronomical Journal*, *156*, 86 (6pp).
- Mishchenko, M. I., Travis, L. D., & Lacis, A. A. (2002). *Scattering, absorption, and emission of light by small particles*. Cambridge university press.
- Muononen, K., & Lumme, K. (1991). Light scattering by solar system dust: the opposition effect and the reversal of polarization. In *Origin and evolution of interplanetary dust* (pp. 159–162). Springer.
- Muslimov, E., Valls-Gabaud, D., Lemaître, G., Hugot, E., Jahn, W., Lombardo, S., Wang, X., Vola, P., & Ferrari, M. (2017). Fast, wide-field and distortion-free telescope with curved detectors for surveys at ultralow surface brightness. *Applied Optics*, *56*, 8639–8647.
- Nakamura, R., & Okamoto, H. (1999). Optical properties of fluffy aggregates as analogue of interplanetary dust particles. *Advances in Space Research*, *23*, 1209–1212.
- Nesvorný, D., Janches, D., Vokrouhlický, D., Pokorný, P., Bottke, W. F., & Jenniskens, P. (2011). Dynamical model for the zodiacal cloud and sporadic meteors. *The Astrophysical Journal*, *743*, 129 (16pp).
- Nesvorný, D., Jenniskens, P., Levison, H. F., Bottke, W. F., Vokrouhlický, D., & Gounelle, M. (2010). Cometary origin of the zodiacal cloud and carbonaceous micrometeorites. Implications for hot debris disks. *The Astrophysical Journal*, *713*, 816–836.

- Van de Noord, E. L. (1970). Observations of the zodiacal light with a balloon-borne telescope. *The Astrophysical Journal*, *161*, 309–316.
- Ootsubo, T., Ueno, M., Ishiguro, M., Usui, F., Pyo, J., Hong, S. S., Kwon, S. M., & Mukai, T. (2009). Mid-Infrared spectrum of the zodiacal light observed with AKARI/IRC. In *AKARI, a Light to Illuminate the Misty Universe* (p. 395). volume 418.
- Pitz, E., Leinert, C., Schulz, A., & Link, H. (1979). Colour and polarization of the zodiacal light from the ultraviolet to the near infrared. *Astronomy & Astrophysics*, *74*, 15–20.
- Pyo, J., Ueno, M., Kwon, S. M., Hong, S. S., Ishihara, D., Ishiguro, M., Usui, F., Ootsubo, T., & Mukai, T. (2010). Brightness map of the zodiacal emission from the AKARI IRC All-Sky Survey. *Astronomy & Astrophysics*, *523*, A53.
- Reach, W. T. (1997). The structured zodiacal light: IRAS, COBE, and ISO observations. In *Diffuse infrared radiation and the IRTS* (p. 33). volume 124.
- Reach, W. T., Kelley, M. S., & Sykes, M. V. (2007). A survey of debris trails from short-period comets. *Icarus*, *191*, 298–322.
- Reach, W. T., Morris, P., Boulanger, F., & Okumura, K. (2003). The mid-infrared spectrum of the zodiacal and exozodiacal light. *Icarus*, *164*, 384–403.
- Renard, J.-B., Levasseur-Regourd, A. C., & Dumont, R. (1995). Properties of interplanetary dust from infrared and optical observations. II. Brightness, polarization, temperature, albedo and their dependence on the elevation above the ecliptic. *Astronomy & Astrophysics*, *304*, 602–608.
- Rosenbush, V., Kolokolova, L., Lazarian, A., Shakhovskoy, N., & Kiselev, N. (2007). Circular polarization in comets: Observations of comet C/1999 S4 (LINEAR) and tentative interpretation. *Icarus*, *186*, 317–330.

- Rowan-Robinson, M., & May, B. (2013). An improved model for the infrared emission from the zodiacal dust cloud: cometary, asteroidal and interstellar dust. *Monthly Notices of the Royal Astronomical Society*, *429*, 2894–2902.
- Sandford, S. A., Aléon, J., Alexander, C. M. O., Araki, T., Bajt, S., Baratta, G. A., Borg, J., Bradley, J. P., Brownlee, D. E., Brucato, J. R., Burchell, M. J., Busemann, H., Butterworth, A., Clemett, S. J., Cody, G., Colangeli, L., Cooper, G., D’Hendecourt, L., Djouadi, Z., Dworkin, J. P., Ferrini, G., Fleckenstein, H., Flynn, G. J., Franchi, I. A., Fries, M., Gilles, M. K., Glavin, D. P., Gounelle, M., Grossemy, F., Jacobsen, C., Keller, L. P., Kilcoyne, A. L. D., Leitner, J., Matrajt, G., Meibom, A., Mennella, V., Mostefaoui, S., Nittler, L. R., Palumbo, M. E., Papanastassiou, D. A., Robert, F., Rotundi, A., Snead, C. J., Spencer, M. K., Stadermann, F. J., Steele, A., Stephan, T., Tsou, P., Tyliczszak, T., Westphal, A. J., Wirick, S., Wopenka, B., Yabuta, H., Zare, R. N., & Zolensky, M. E. (2006). Organics Captured from Comet 81P/Wild 2 by the Stardust Spacecraft. *Science*, *314*, 1720–1724. URL: <http://science.sciencemag.org/content/314/5806/1720>. doi:10.1126/science.1135841.
- Schuerman, D. W. (1979). Inverting the zodiacal light brightness integral. *Planetary and Space Science*, *27*, 551–556.
- Skomorovsky, V. I., Trifonov, V. D., Mashnich, G. P., Zagaynova, Y. S., Fainshtein, V. G., Kushtal, G. I., & Chuprakov, S. A. (2012). White-light observations and polarimetric analysis of the solar corona during the eclipse of 1 August 2008. *Solar Physics*, *277*, 267–281.
- Sparrow, J. C., & Ney, E. P. (1972). Observations of the Zodiacal Light from the Ecliptic to the Poles. *The Astrophysical Journal*, *174*, 705–716.

- Staude, J., & Schmidt, T. (1972). Circular polarisation measurements of the zodiacal light. *Astronomy & Astrophysics*, *20*, 163–164.
- Sykes, M. V. (1988). IRAS observations of extended zodiacal structures. *The Astrophysical Journal*, *334*, L55–L58.
- Sykes, M. V., & Walker, R. G. (1992). Cometary dust trails: I. Survey. *Icarus*, *95*, 180–210.
- Umow, v. N. (1905). Chromatische depolarisation durch lichtzerstreuung. *Phys. Z*, *6*, 674–676.
- Valls-Gabaud, D., & collaboration, M. (2016). The MESSIER surveyor: unveiling the ultra-low surface brightness universe. *Proceedings of the International Astronomical Union*, *11*, 199–201.
- Weinberg, J. L. (1964). The zodiacal light at 5300 Å. In *Annales d’Astrophysique* (p. 718). CNRS volume 27.
- Weinberg, J. L. (1985). Zodiacal light and interplanetary dust. In *International Astronomical Union Colloquium* (pp. 1–6). Cambridge University Press volume 85.
- Weinberg, J. L., & Hahn, R. C. (1980). Brightness and Polarization of the Zodiacal Light: Results of Fixed-Position Observations from Skylab. In *Symposium-International Astronomical Union* (pp. 19–22). Cambridge University Press volume 90.
- Weinberg, J. L., & Mann, H. M. (1968). Negative polarization in the zodiacal light. *The Astrophysical Journal*, *152*, 665–666.
- Weinberg, J. L., & Sparrow, J. G. (1978). Zodiacal light as an indicator of interplanetary dust. *Cosmic dust*, (pp. 75–122).

- Whipple, F. L. (1950). A comet model. I. The acceleration of Comet Encke. *The Astrophysical Journal*, 111, 375–394.
- Wolstencroft, R. D., & Kemp, J. C. (1972). Circular polarization of the night sky radiation. *The Astrophysical Journal*, 177, L137–L140.
- Wolstencroft, R. D., & Rose, L. J. (1967). Observations of the zodiacal light from a sounding rocket. *The Astrophysical Journal*, 147, 271–292.
- Wright, A. W. (1874). On the Polarization of the zodiacal Light. *American Journal of Science and Arts*, VII, 451–458.
- Yang, H., & Ishiguro, M. (2015). Origin of interplanetary dust through optical properties of zodiacal light. *The Astrophysical Journal*, 813, 87 (9pp).
- Yang, H., & Ishiguro, M. (2018). Evolution of cometary dust particles to the orbit of the Earth: Particle size, shape, and mutual collisions. *The Astrophysical Journal*, 854, 173 (14pp).
- Yang, H., Ishiguro, M., Usui, F., & Ueno, M. (2012). High-Resolution Map of Zodiacal Dust Bands by WIZARD Measurements. In *Asteroids, Comets, Meteors 2012*. volume 1667.



Figure 1: Zodiacal light seen from Paranal, Chile. The bright planet at the top center is Jupiter (ESO/Y.Beletsky).

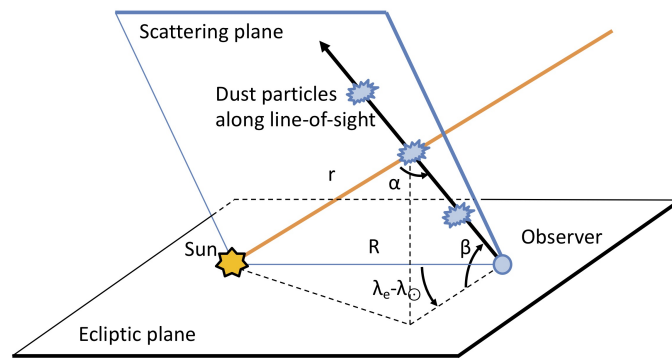


Figure 2: Zodiacal light geometry of observation in helio-ecliptic coordinates.

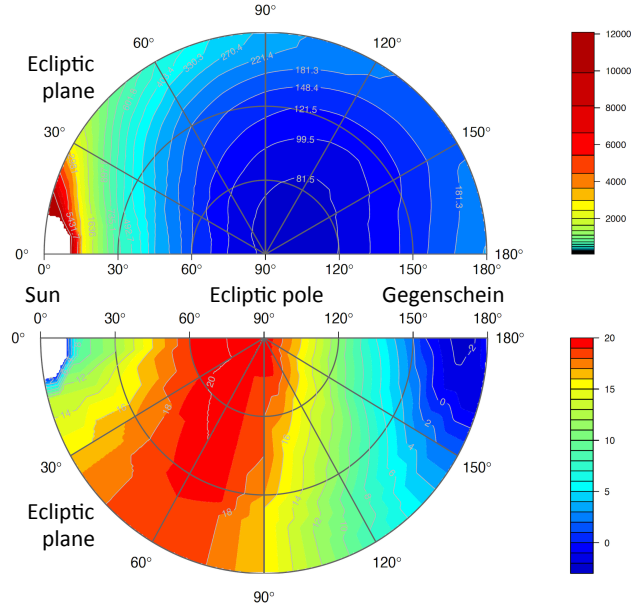


Figure 3: Upper part: Map of the zodiacal light brightness ($10^{-8} \text{ W m}^{-2} \text{ sr}^{-1} \mu\text{m}^{-1}$) at 550 nm. Lower part: Map of the zodiacal linear polarization (in percent). The outer circle represents the ecliptic, the point at 0° is the Sun, the central point is the ecliptic pole, and the near 180° region is the Gegenschein, with an increase in brightness by backscattering, and a low and even negative linear polarization between 160° and 180° . Values are corrected for oscillations induced by the slight inclination of the zodiacal light symmetry plane and the Earth's orbit eccentricity. Based on data from Levasseur-Regourd & Dumont (1980); Levasseur-Regourd (1996) and Leinert et al. (1998); updated from Lasue et al. (2015); Levasseur-Regourd & Lasue (2019).

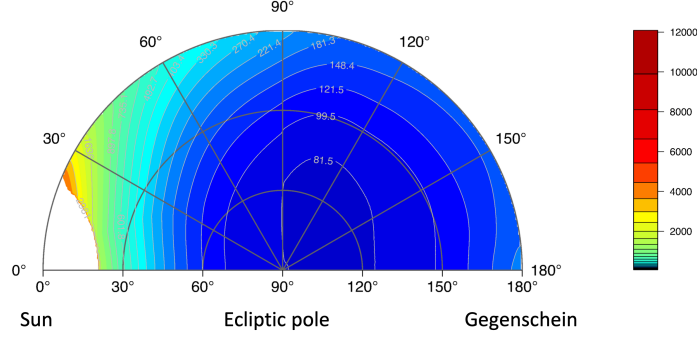


Figure 4: Most recent map of the zodiacal light brightness ($10^{-8} \text{ W m}^{-2} \text{ sr}^{-1} \mu\text{m}^{-1}$). Brightness levels are comparable to those presented in the upper part of Fig. 3, while the resolution is significantly improved. The outer circle represents the ecliptic, the point at 0° is the Sun, the central point is the ecliptic pole, and the near 180° region is the Gegenschein. Based on data from Buffington et al. (2016) and adapted from (Levasseur-Regourd & Lasue, 2019).

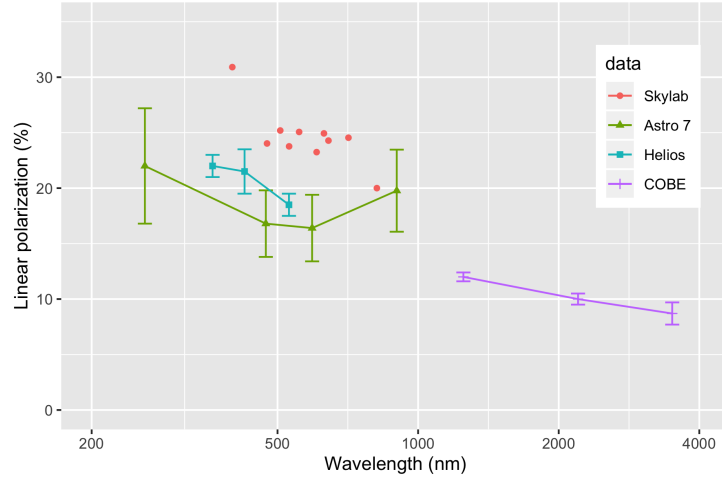


Figure 5: Wavelength variation of the linear polarization, P , in different directions of the sky. Skylab at the North Celestial Pole (Weinberg & Hahn, 1980); rocket Astro 7 ($\lambda_e - \lambda_\odot = 25^\circ$) (Pitz et al., 1979); Helios ($\lambda_e - \lambda_\odot = 90^\circ$) (Leinert et al., 1982); COBE ($\lambda_e - \lambda_\odot = 90^\circ$) (Berriman et al., 1994).

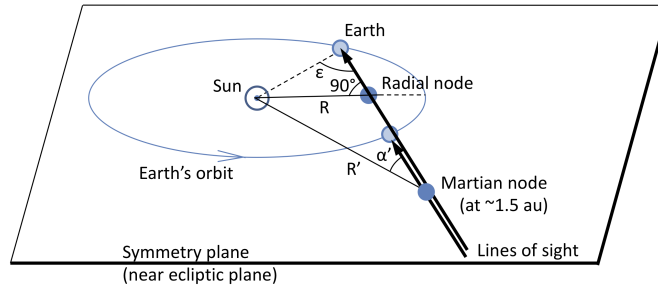


Figure 6: Geometry of observations for inversion of the zodiacal light, for lines of sight in the symmetry plane (near the ecliptic) of the zodiacal cloud (Figure adapted from Renard et al., 1995). Note that these regions correspond to places where mathematical inversion of the line-of-sight integral is possible with minimal assumptions, and not where measurements were made. See text for additional details.

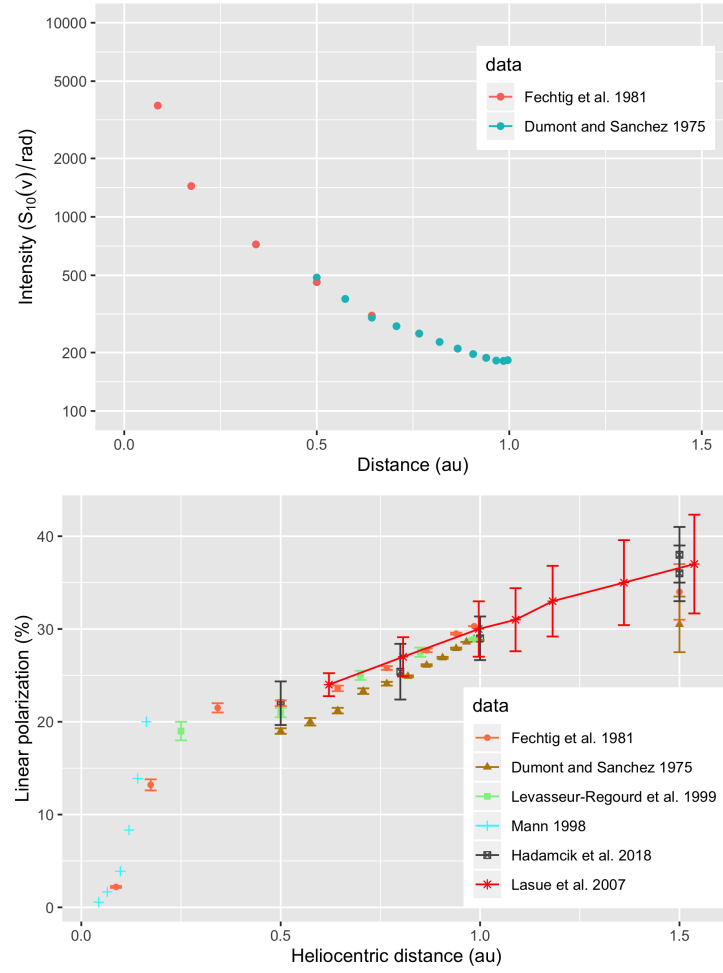


Figure 7: Variation of the local near-ecliptic brightness (top) and linear degree of polarization, P , (in percent, bottom), at 90° phase angle as a function of the heliocentric distance (au), adapted from Dumont & Sanchez (1975b); Fechtig et al. (1981); Levasseur-Regourd (1996); Mann (1998); Hadamcik et al. (2018); Lasue et al. (2007) and references within.

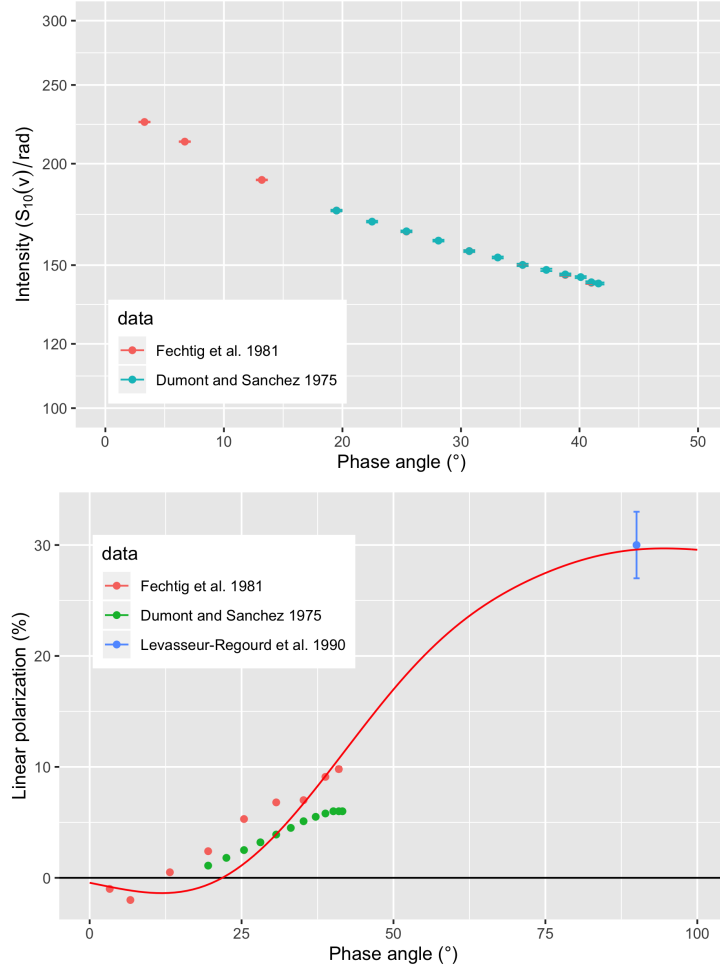


Figure 8: Phase curves of the local near-ecliptic brightness (top) and linear degree of polarization, P , (in percent bottom), at 1.5 au, adapted from Dumont & Sanchez (1975b); Fechtig et al. (1981); Levasseur-Regourd et al. (1990) and references within.